Supporting Information

The Internal Dynamics of Mini c TAR DNA Probed by EPR of Nitroxide Spin Labels at the Lower Stem, the Loop, and the Bulge

Yan Sun,[§] Ziwei Zhang,[‡,¶] Vladimir M. Grigoryants,[§] William K. Myers,[§,+] Fei Liu,[§] Keith A Earle,[#] Jack H. Freed,[‡] and Charles P. Scholes*[,§]

[§]Department of Chemistry, University at Albany, 1400 Washington Avenue, Albany, NY 12222

[‡]Department of Chemistry and Chemical Biology and ACERT, Cornell University, Ithaca, NY 14853

[#]Department of Physics, University at Albany, 1400 Washington Avenue, Albany, NY 12222

[†] This work was supported by the NIH (GM066253-01A1 and 3RO1GM06625304S1 to C.P.S., NIH/NCRR Grant P41RR016292 and NIH/NIGMS Grant P41GM103521 to J.H. F.) and an RNA Institute Interdisciplinary Pilot Research Program 2010 Award, UAlbany to K.A.E.

*Corresponding Author: Charles P. Scholes. Telephone: 518-442-4551, Fax: 518-442-3462, Email: cps14@albany.edu.

[¶]Current Address: State Key Laboratory of Magnetic Resonance and Atomic and Molecular Physics, Wuhan Institute of Physics and Mathematics, Chinese Academy of Sciences, Wuhan, Hubei 430071 (China)

[+]Current Address: Department of Chemistry, University of California, 1 Shields Avenue, Davis, California 95616

Table of Contents

Method 1 – Labeling phosphorothioate linkages. Per **Scheme 1** in the main text, 100 nmoles of phosphorothioate-modified mini c TAR DNA were mixed with a 60 mM solution of 3-(2-iodoacetamido)-proxy or 3-Iodomethyl- (1-oxy-2,2,5,5-tetramethylpyrroline) in a 100 μl volume. This volume contained a solution of 100 mM MES [2-(N-Morpholino)-ethanesulfonic Acid (pH 5.8)] and either 20% (v/v) acetonitrile when using 3-Iodomethyl-(1-oxy-2,2,5,5-tetramethylpyrroline) or 50% formamide when using of 3-(2-iodoacetamido)-proxyl. These solutions thus contained a 60-fold molar excess of spin probe to mini c TAR DNA. The reaction was allowed to proceed in the dark with continuous shaking for 24 h at room temperature. The reaction mixtures were first subjected to anion-exchange HPLC using a PA-100 column (4X250mm2, Dionex Inc., Sunnyville, CA). Oligonucleotides were eluted using a low salt stationary phase (buffer A: 1 mM $NaClO_4$, 20 mM Tris–HCl, pH 6.8 and 20% v/v acetonitrile) and a high salt mobile phase (buffer B: 400 mM $NaClO_4$, 20 mM Tris–HCl, pH 6.8 and 20% v/v acetonitrile). The presence of oligonucleotides of different sizes and the separation of labeled samples were detected via absorbance at 260 nm, as shown in **Figure 1S.** It is possible that the double peak from the FPLC trace of unlabled TAR in **Figure 1S** is due to previously reported Rp/Sp diastereomers of the phosphorothioate (*1*). With the concentrations of mini TAR used for our preparative FPLC we did not routinely resolve RpSp differences and we did not selectively purify oligonucleotide samples with separate Rp or Sp conformers. A denaturing gel, showing separation of phosphorothioate-labeled and unlabeled mini c TAR DNA, is provided in **Figure 2**S.

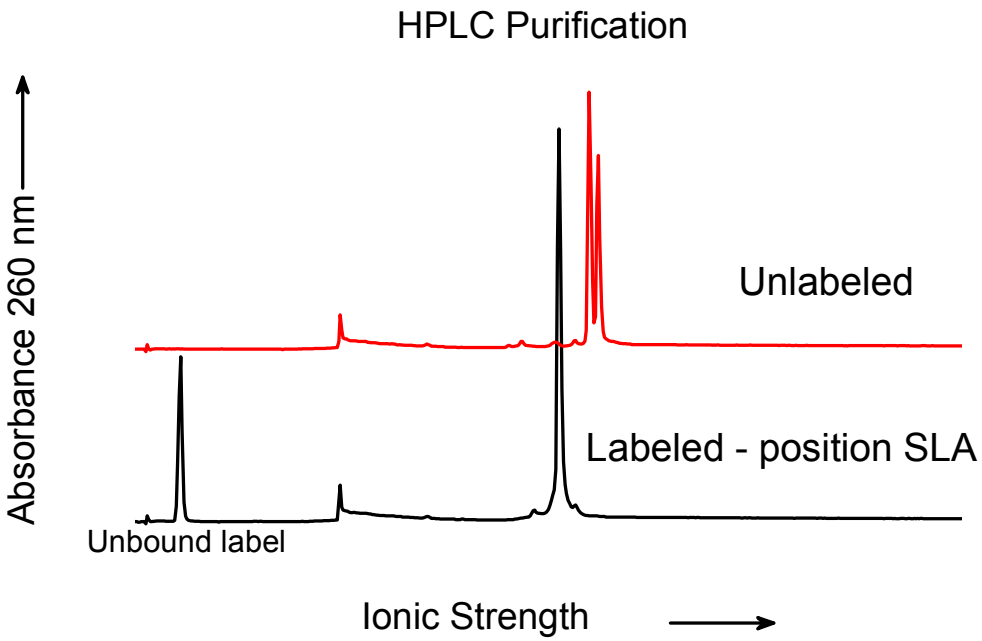

Figure 1S. UV-detected output of HPLC purification for SLA-labeled mini c TAR DNA.

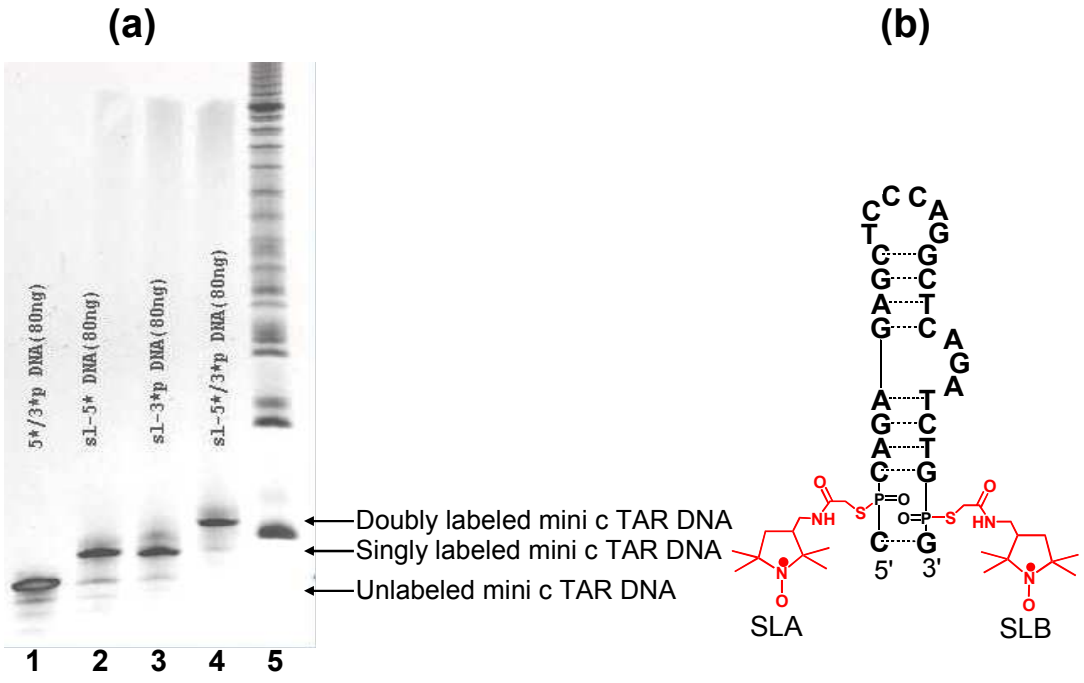

Figure 2S. **(a)** Analytical gel results showing SLA, SLB, SLAB bands before and after spin label reaction. **Lane 1**: unlabeled mini c TAR DNA (3.0 pmoles), **lane 2**: SLA reaction mixture, **lane 3**: SLB reaction mixture, **lane 4**: SLAB reaction mixture (double labeled) (3.0 pmoles), **lane 5**: 10 bp DNA ladder. **b**) Phosphorothioate labeling sites, SLA and SLB on mini c TARDNA. The lowest ladder band is from 30 bases.

Method 2 - Preparation of spin-labeled mini c TAR DNA via the reaction of 2′-amino-2′-deoxycytidine and 4-Isocyanato-2, 2, 6, 6-tretramethylpiperidine 1-oxyl. As shown in **Scheme 2** in the main text this spin label reaction was conducted as follows: 27-mer mini c TAR DNA containing a 2'-amino cytidine (20 µL, 2 mM) in 70 mM boric acid buffer, pH 8.6, was treated with 12 µL of -8 °C precooled formamide (*2*). To the resulting solution was added 10 µL of 200 mM 4-Isocyanato TEMPO in DMF at -8 °C. The solution was mixed and incubated at -8 °C for 1 h. The excess nitroxide was removed by denaturing PAGE gel[1] **Figure 3S** or anion exchange HPLC.

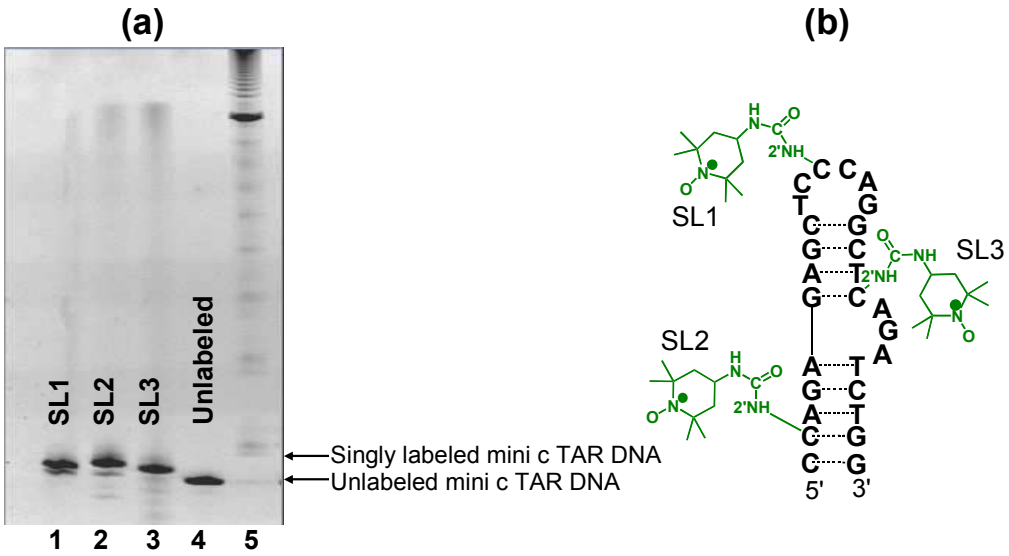

Figure 3S. (**a**): Analytical gel for spin label reaction of mini c TAR DNA. **Lane 1**: SL1 (Loop region), 3.0 pmole; **lane 2**: SL2 (Stem region), 3.0 pmole; **lane 3**: SL3 (Bulge region), 3.0 pmole; **lane 4**, unlabeled mini c TAR DNA; **lane 5**: 10 bp DNA ladder. Arrows indicate the spin labeled mini c TAR DNA band and the unlabeled mini c TAR DNA band. (**b**) 2' Amino labeling sites, SL1, SL2, SL3 on mini c TAR DNA. The lowest ladder band is from 30 bases.

[1]The PAGE evidence is for a single distinct band that moves more slowly than unreacted mini c TAR DNA. That band definitely had spin labeled material. However, the product collected from the desired eluted band contained only 40 % of the expected spin concentration, based on the ratio of spin concentration from EPR double integration to the optical absorbance of the mini c TAR DNA. The yield of paramagnetic nitroxide was improved by eliminating unreacted polymerization initiation chemicals by using a minimal amount of polymerization reagent, by doing the gel polymerization a day in advance of use, and by pre-running the gel for three hours to wash out unreacted polymerization initiation chemicals.

Non-Denaturing gel shift assays. The purpose of these assays was to determine the similarity between the binding of NCp7 to the unlabeled and the binding of NCp7 to labeled forms of mini c TAR DNA. These assays were performed in 50 mM Hepes buffer, pH 7.5, with a 15% cross-linked polyacrylamide gel (Biorad). The reaction mixture of mini c TAR DNA and NCp7 was incubated initially at room temperature for about 15 minutes. Titrations were performed at a constant mini c TAR DNA concentration of 1.4 μM, and gels were run at 4 ºC. SYBERGold Nucleic acid gel stain solution (Invitrogen, Cat#: S-11494) was used for gel staining and images were observed by a FOTO/UV21 apparatus. **Figure 4S** provides a comparison of the NCp7 binding patterns at increasing ratios of NCp7 to unlabeled or labeled mini c TAR DNA. At a low ratio of NCp7 to mini c TAR DNA a complex of DNA and NCp7 appeared at a position similar to the 30 bp marker, and this is indicated as a 1:1 nucleoprotein complex; such a band was also found under similar gel conditions in previous work on spin labeled ψ_3 RNA (*3*). At a higher ratio of NCp7 to mini c TAR DNA a more diffuse, slowly moving, apparently higher molecular weight mass appeared, and it is indicated in **Figure 4S** as a higher order NCp7/mini c TAR DNA complex. Such complexes have also been observed by others through gel shift assays (*4*). Also, at higher ratios of NCp7 to mini c TAR DNA, there was evidence for an uncharged or positively charged complex which forms at the top of the gel and which does not travel into the gel. We emphasize that there was little difference in the gel patterns between the unlabeled and labeled mini c TAR DNA. This similarity suggests that the spin probe does not interfere with the NCp7- mini c TAR DNA binding.

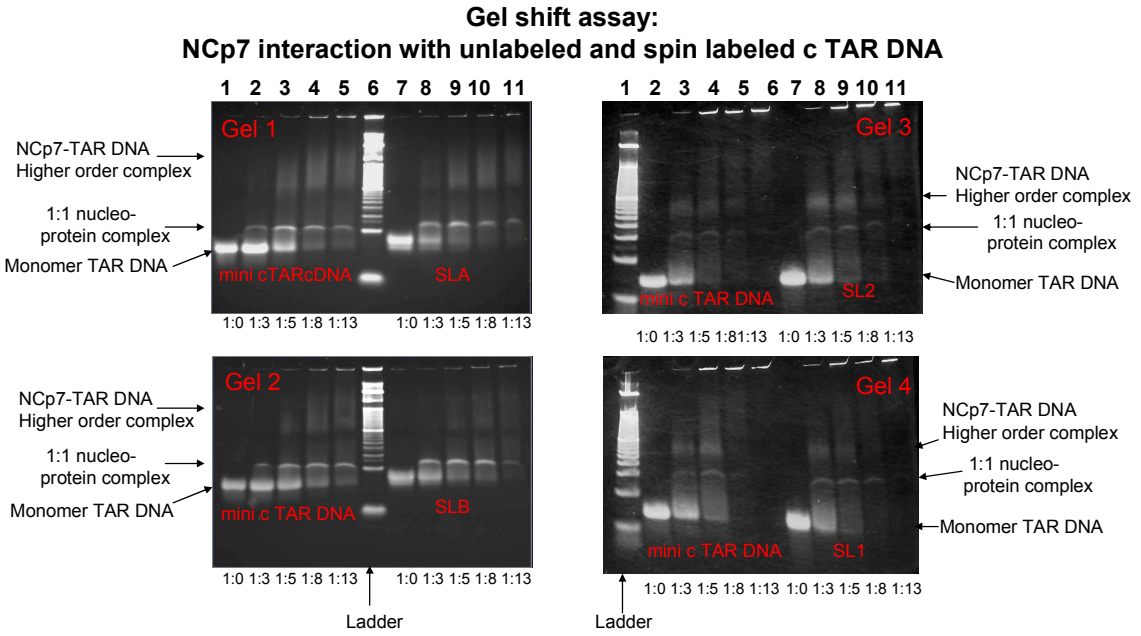

Figure 4S. Non-denaturing gel assay comparison between the interaction of NCp7 with mini c TAR DNA and the interaction of NCp7 with spin labeled mini c TAR DNA.

Gel 1: Comparison of unlabeled mini c TAR DNA with SLA stem-labeled mini c TAR DNA.
Gel 2: Comparison of unlabeled mini c TAR DNA with SLB stem-labeled mini c TAR DNA.

For gels 1 and 2, the identities of lanes are: Lane 1 -Free mini c TAR DNA; from Lane 2 - Lane 5 the mini c TAR DNA/NCp7 ratio decreases from 1:3, 1:5, 1:8, to 1:13, respectively. Lane 6, 10 bp DNA ladder. Then Lane 7 - spin labeled mini c TAR DNA. From Lane 8 - Lane 11 the spin labeled mini c TAR DNA/NCp7 ratio decreases from 1:3, 1:5, 1:8, to 1:13, respectively

Gel 3: Comparison of unlabeled mini c TAR DNA with SL2 stem-labeled mini c TAR DNA.
Gel 4. Comparison of unlabeled mini c TAR DNA with SL1 stem-labeled mini c TAR DNA.

For gels 3 and 4, the identities of lanes are: Lane 1, 10 bp DNA ladder, Lane 2 --Free mini c TAR DNA; from Lane 3 - Lane 6 the mini c TAR DNA/NCp7 ratio decreases from 1:3, 1:5, 1:8, to 1:13, respectively. Then Lane 7 - spin labeled mini c TAR DNA. From Lane 8 - Lane 11 the spin labeled mini c TAR DNA/NCp7 ratio decreases from 1:3, 1:5, 1:8, to 1:13, respectively

.

Melting of labeled and unlabeled mini c TAR DNA. Melting was followed by monitoring hyperchromic absorbance changes at 260 nm using the UV-Melts technique (*5*). Absorption spectra (Cary 3 UV-Vis Spectrophotometer equipped with thermostatted Peltier temperature controller) were recorded as a function of temperature at 260 nm. The temperature controller was ramped at a rate of 0.3 ^{o}C per minute from 20-95 ^{o}C. The melting temperatures were followed in 50 mM HEPES buffer, pH 7.5, in the presence and the absence of 0. 2 mM $MgCl_2$ at a mini c TAR DNA concentration of 2.0 μM. The melting profile was obtained from the first derivative of the absorbance with respect to the temperature. Then, using previously developed non-linear least-squares fitting software (*5*), thermodynamic parameters (T_m, ΔH, ΔS, ΔG) were derived from the fit of spectroscopic data to a two-state melting model.

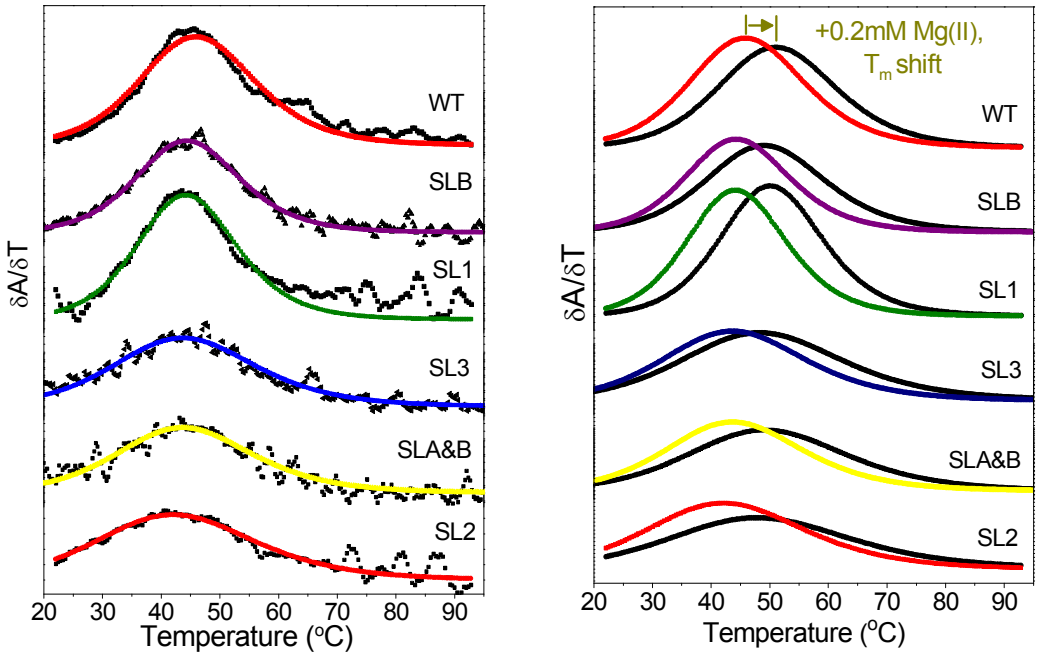

Figure 5S. Melting profiles (δA/δT at 260 nm) for wild type and labeled mini c TAR DNA. The figure on the left was obtained from 2 μM mini c TAR DNA in 50 mM HEPES, pH 7.5. The figure on the right was obtained from 2 μM mini c TAR DNA in 50 mM HEPES, pH 7.5, with 0.2 mM $MgCl_2$.

Table 1S.
Thermodynamic parameters from UV-Melting Profiles of for unlabeled mini c TAR DNA, SL1, SL2, SL3, SLB, and SLAB

Buffer \ DNA		WT	SLB	SLAB	SL1	SL2	SL3
50mM Hepes, pH 7.5	T_m(°C)	43.4	44.7	44.4	44.6	43.1	44.5
	ΔH (Kcal/mol)	-36.9	-34.1	-25.7	-35.4	-21.9	-24.7
	ΔS (Kcal/mol.K)	0.117	0.107	0.081	0.112	0.069	0.078
	$\Delta G_{20°C}$ (Kcal/mol)	-2.7	-2.7	-2.0	-2.7	-1.6	-1.9
	$\Delta G_{37°C}$ (Kcal/mol)	-0.8	-0.8	-0.6	-0.7	-0.4	-0.6
50mM Hepes, 0.2mM $MgCl_2$ pH 7.5	T_m(°C)	49.6	49.6	50.1	50.6	49.2	49.3
	ΔH (Kcal/mol)	-32.6	-30.4	-22.8	-35.7	-20.0	-22.5
	ΔS (Kcal/mol.K)	0.101	0.094	0.071	0.110	0.062	0.070
	$\Delta G_{20°C}$ (Kcal/mol)	-3.0	-2.8	-2.1	-3.4	-1.8	-2.1
	$\Delta G_{37°C}$ (Kcal/mol)	-1.3	-1.2	-0.9	-1.5	-0.8	-0.9

Mg^{2+} stabilized the secondary structure of unlabeled mini c TAR DNA, SL1 (loop region) , SL2 (stem region), SL3 (bulge region), SLB (3' end) and SLAB (5'/3' end). The presence of spin label probes on different sites caused only slight T_m changes, less than 1.0 °C. However a comparison of enthalpy (ΔH) and entropy values (ΔS), showed that labels SL2, SL3 and SLAB caused a destabilizing increase in ΔH that was approximately 10 Kcal/mol, where this increase was offset by a compensating decrease in entropy of melting. As estimated from free energy of melting $\Delta G_{20\text{-}C}$ (= ΔH – 293ΔS), the SL2, SL3, and SLAB (5'/3' ends) were less stable than SL1, SLB and unlabeled mini c TAR DNA by about 1 Kcal/mol at 20 ºC. The implication is that the labels showing diminished enthalpy interfere with base stacking and hydrogen bonding, possibly through perturbation of sugar pucker and rotation angles. We note that double

labels of the iodomethyl-phosphorothioate variety have typically shown little perturbation to duplex DNA structures (*6*) although the SLAB bi-label here did perturb the enthalpy.

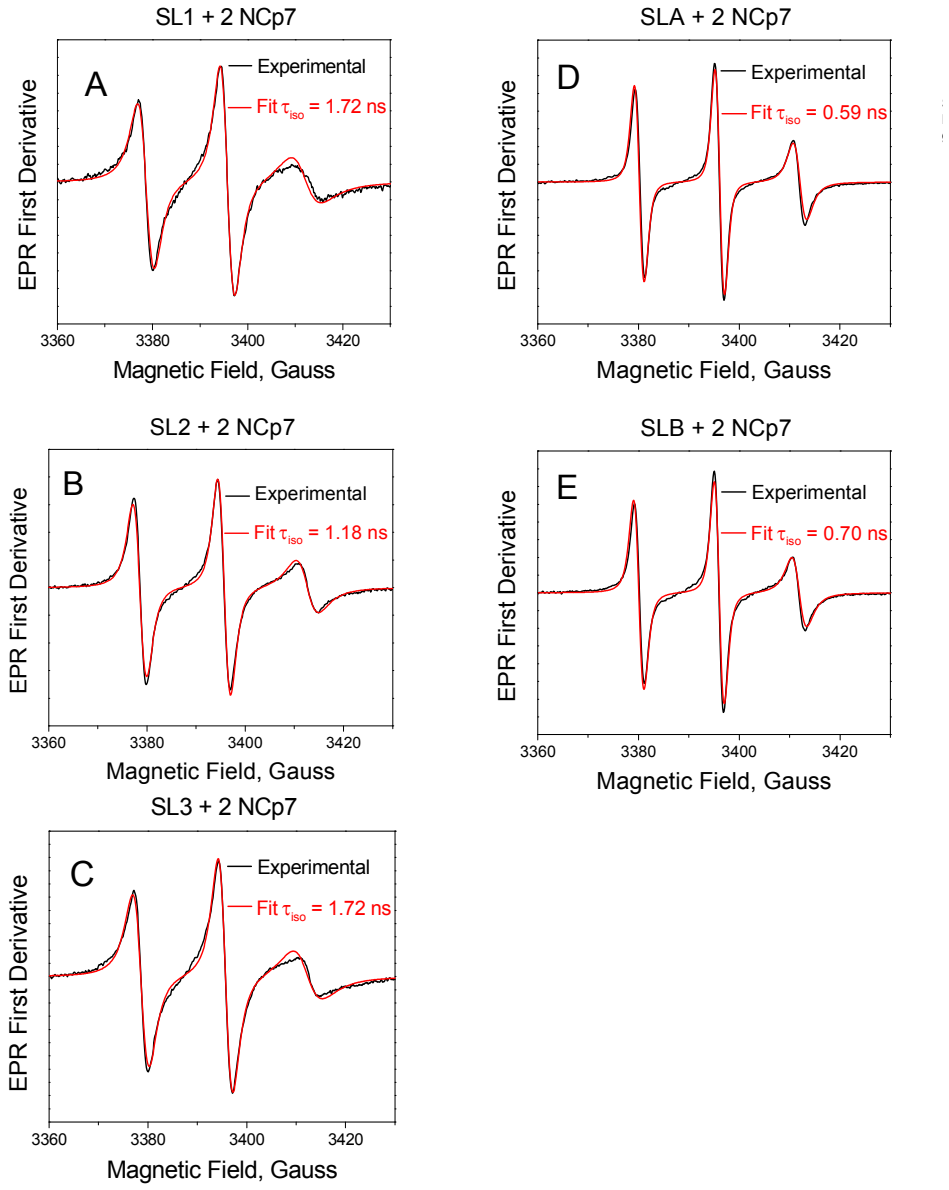

Figure 6S. This figure compares simulated X-band EPR spectra from SL1, SL2, SL3, SLA, and SLB to experimental spectra obtained in the presence of a two-fold excess of NCp7. The simulated spectra were fit using the NLSL routine (*7*) with an isotropic correlation time τ_{iso}.

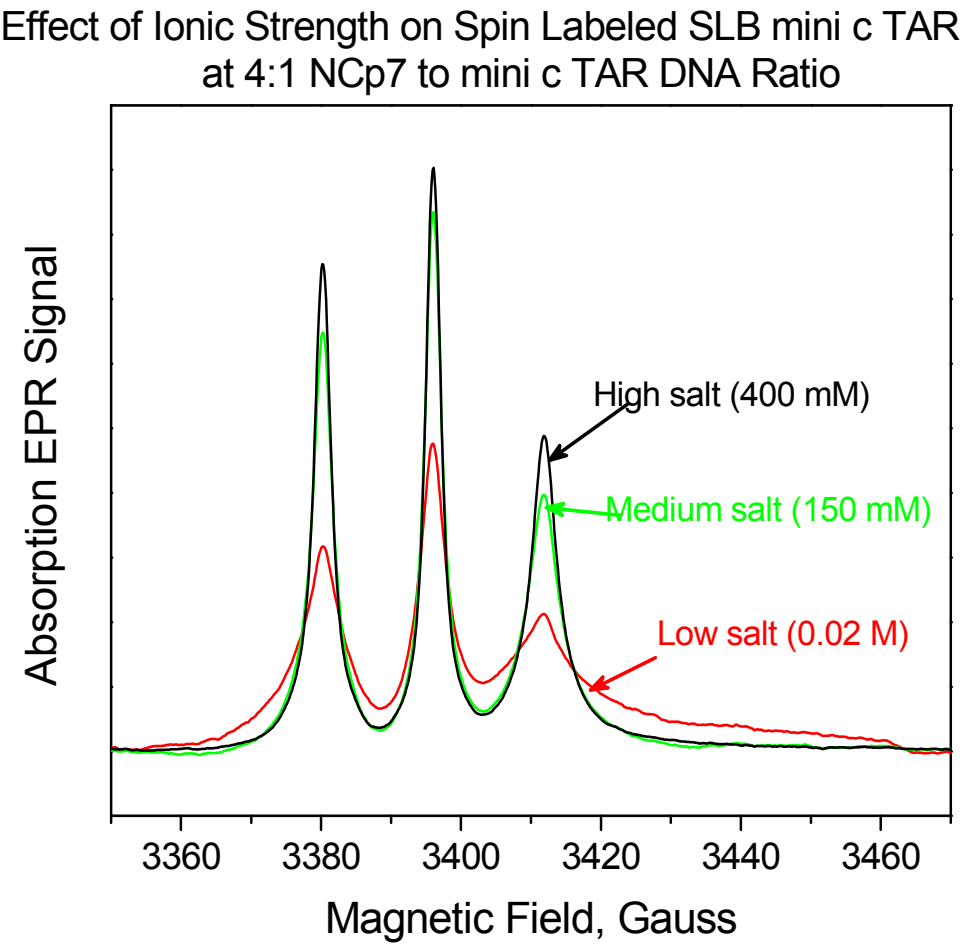

Figure 7S. This figure compares the integrated X-band line shapes of mini c TAR DNA labeled at position SLB at the 5' terminal when there was a 4:1 ratio of NCp7:mini c TAR DNA under conditions of increasing ionic strength. The lowest concentration salt spectrum showed a major component with tumbling time greater than 5 ns. The isotropic tumbling time with 0.15 M NaCl was 0.86 ns, and the isotropic tumbling time at 0.4 M NaCl was 0.66 ns. Spectra were normalized on the second integral. The buffer conditions were: 20mM Hepes, variable NaCl, 0.2 mM $MgCl_2$, pH = 7.5.

Motion of spin labeled c TAR DNA studied by high-field, high-frequency EPR, where axial symmetry is assumed for the local probe diffusion tensor and rhombic symmetry for the restraining potential. In the main text SRLS simulations (by what we call Method 1) were performed using a rhombic diffusion tensor ($\underline{\mathfrak{R}}_x \neq \underline{\mathfrak{R}}_y \neq \underline{\mathfrak{R}}_z$ and $\underline{\mathfrak{R}}_x \sim \underline{\mathfrak{R}}_y >> \underline{\mathfrak{R}}_z$) and an axial order parameter $\mathbf{c}_{20}$. Comparable fits (by what we call Method 2) , shown here in **Figure 8S**, were obtained with an axial diffusion tensor $\underline{\mathfrak{R}}_\perp >> \underline{\mathfrak{R}}_\parallel$ and at least two restraining potential parameters, $\mathbf{c}_{20}$ and $\mathbf{c}_{22}$. $\mathbf{c}_{22}$ shows rhombicity in the ordering, and it is necessary for good fits to the 9.5 GHz and 236.6 GHz spectra of SL1, SL2, and SL3 for Method 2. As indicated in **Table 2S**, the values of S_{22} [$S_{22} = (2/3)^{1/2}(S_{xx}-S_{yy})$] are negative (-0.26 – -0.27), indicating the non-axial preference in ordering along the y-axis. However, this fitting was unstable unless $\underline{\mathfrak{R}}_\parallel$ was preset and at least in the case of SL1, W_{240} needed to be preset at a rather low value. Thus, we regard the fit in Table 1 as the more reliable. Indeed, it is reasonable to expect that EPR experiments obtained at more frequencies (*8*) will be helpful to resolve such uncertainties.

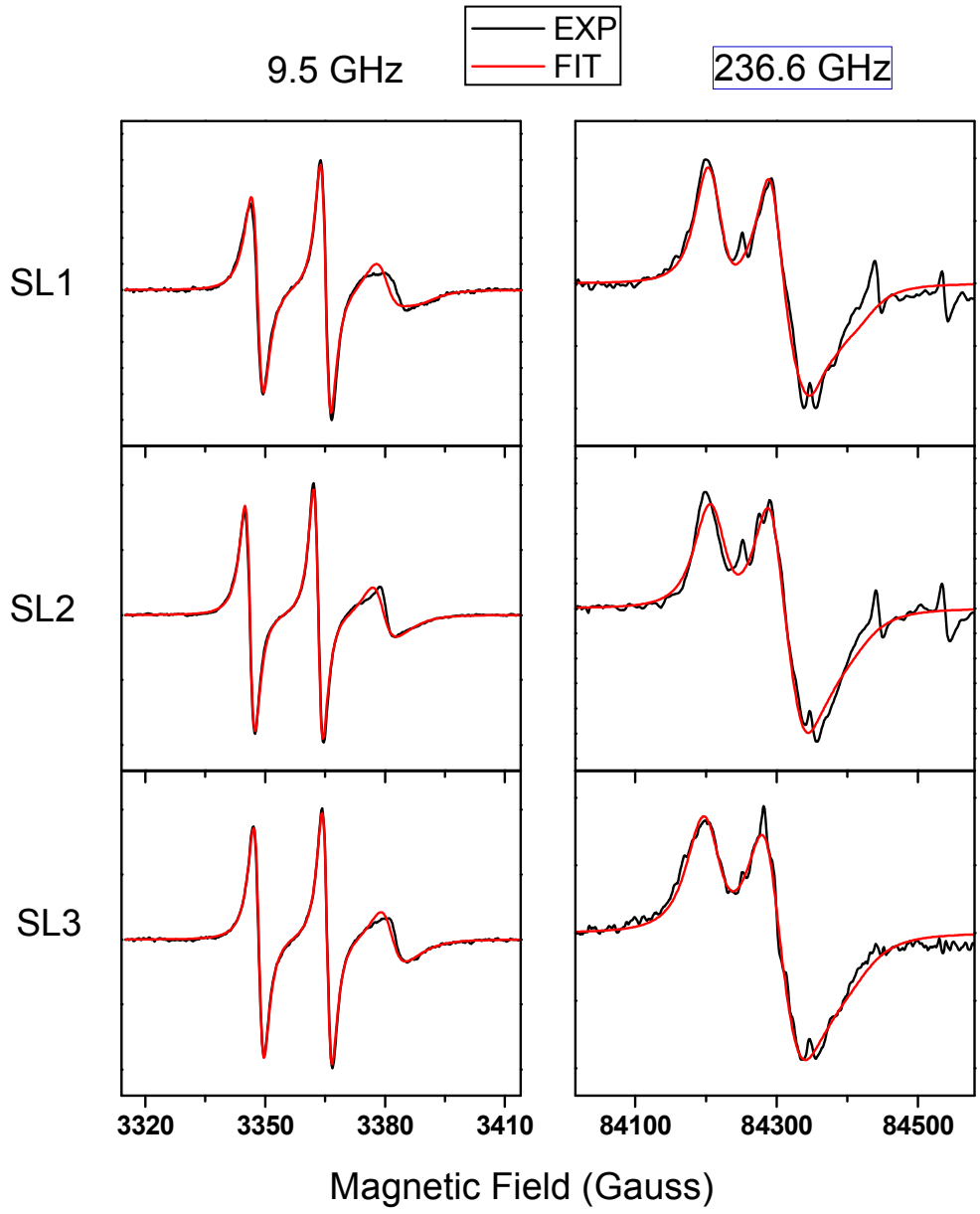

Figure 8S. This figure shows the combined fitting to 9.5 GHz and 240 GHz spectra to provide evidence for anisotropic diffusion tensor of probe provided through parameters for SL1, SL2, and SL3 in the following Table 2S. $\underline{\mathfrak{R}}_{\perp}$, $\underline{\mathfrak{R}}_{\|}$, $\mathbf{c}_{20}$, $\mathbf{c}_{22}$, and $\underline{\mathfrak{R}}_{c}$ are major fitting parameters.

Table 2S: Fitting Parameters for Simultaneous 9.5 - 236.6 GHz Fitting to the EPR Spectra of SL1, SL2, and SL3. . $\underline{\mathfrak{R}}_{\perp}$, $\underline{\mathfrak{R}}_{7}$, $\mathbf{c}_{20}$, $\mathbf{c}_{22}$, and $\underline{\mathfrak{R}}_{c}$ are major fitting parameters.

Spin Label	SL1	SL2	SL3
$\underline{\mathfrak{R}}_{c}$ (10^7 s^{-1})	2.0	2.6	2.8
$\underline{\mathfrak{R}}_{\perp}$ (10^7 s^{-1})	35.5	39.3	35.5
$\underline{\mathfrak{R}}_{\parallel}$ (10^7 s^{-1})	0.3 fixed[a]	0.3 fixed[a]	0.3 fixed[a]
$\mathbf{c}_{20}$ / $\mathbf{c}_{22}$	2.45 / -1.77	2.22 / -1.65	2.36 / -1.74
S_{20} / S_{22}	0.40 / -0.26	0.37 / -0.27	0.39 / -0.27
$W_{9\ GHz}$ (G)	0.84	0.81	0.79
$W_{240\ GHz}$ (G)	0.1 fixed[b]	2.9	6.8

[a] $\underline{\mathfrak{R}}_{\parallel}$ goes to an unreasonable low value (even slower than the rigid limit tumbling rate) in the simulation if not fixed.

[b] $W_{240\ GHz}$ for SL1 goes to a negative value if not fixed to a small positive value 0.1 Gauss.

References

(1) Grant, G. P., Popova, A., and Qin, P. Z. (2008) Diastereomer characterizations of nitroxide-labeled nucleic acids. *Biochem Biophys Res Commun 371*, 451-455.

(2) Edwards, T. E., Okonogi, T. M., Robinson, B. H., and Sigurdsson, S. T. (2001) Site-specific incorporation of nitroxide spin-labels into internal sites of the TAR RNA; structure-dependent dynamics of RNA by EPR spectroscopy. *J Am Chem Soc 123*, 1527-1528.

(3) Xi, X., Sun, Y., Karim, C. B., Grigoryants, V. M., and Scholes, C. P. (2008) HIV-1 nucleocapsid protein NCp7 and its RNA stem loop 3 partner: rotational dynamics of spin-labeled RNA stem loop 3. *Biochemistry 47*, 10099-10110.

(4) Bazzi, A., Zargarian, L., Chaminade, F., Boudier, C., De Rocquigny, H., Rene, B., Mely, Y., Fosse, P., and Mauffret, O. (2011) Structural insights into the cTAR DNA recognition by the HIV-1 nucleocapsid protein: role of sugar deoxyriboses in the binding polarity of NC. *Nucleic Acids Res 39*, 3903-3916.

(5) Theimer, C. A., Wang, Y., Hoffman, D. W., Krisch, H. M., and Giedroc, D. P. (1998) Non-nearest neighbor effects on the thermodynamics of unfolding of a model mRNA pseudoknot. *J Mol Biol 279*, 545-564.

(6) Popova, A. M., Kalai, T., Hideg, K., and Qin, P. Z. (2009) Site-specific DNA structural and dynamic features revealed by nucleotide-independent nitroxide probes. *Biochemistry 48*, 8540-8550.

(7) Budil, D. E., Lee, S., Saxena, S., and Freed, J. H. (1996) Nonlinear-Least-Squares Analysis of Slow-Motion EPR Spectra in One and Two Dimensions Using a Modified Levenberg-Marquardt Algorithm. *J. Magn. Reson., Ser. A 120*, 155-189.

(8) Zhang, Z., Fleissner, M. R., Tipikin, D. S., Liang, Z., Moscicki, J. K., Earle, K. A., Hubbell, W. L., and Freed, J. H. (2010) Multifrequency electron spin resonance study of the dynamics of spin labeled T4 lysozyme. *J Phys Chem B 114*, 5503-5521.